

## Double photon production in polarized proton-proton collisions

M. A. Doncheski

*Department of Physics, University of Wisconsin, Madison, Wisconsin 53706*

R. W. Robinett

*Department of Physics, The Pennsylvania State University, University Park, Pennsylvania 16802*

(Received 6 January 1992)

We derive the partonic level longitudinal spin-spin asymmetries for the processes relevant to the hadronic production of isolated double photon events, specifically  $q\bar{q} \rightarrow \gamma\gamma$  and  $gg \rightarrow \gamma\gamma$ . We discuss production rates and observable asymmetries ( $A_{LL}$ ) in polarized  $pp$  collisions at the BNL Relativistic Heavy Ion Collider and their dependence on the spin-dependent sea and gluon distributions. Because the decay  $H^0 \rightarrow \gamma\gamma$  is a possibly important signal for intermediate mass Higgs-scalar production, we also briefly discuss the spin dependence of standard model Higgs-boson production via  $gg \rightarrow H^0$  (low  $p_T$ ) and  $gg \rightarrow gH^0$ ,  $qg \rightarrow qH^0$ , and  $q\bar{q} \rightarrow gH^0$  (high  $p_T$ ).

PACS number(s): 13.88.+e, 12.38.Bx, 13.85.Qk, 14.80.Gt

Recent machine studies [1–3] have indicated that, using the now tested [4] technology of Siberian snakes, it will be feasible to achieve high luminosity ( $\mathcal{L}$  up to  $2 \times 10^{32} \text{ cm}^{-2} \text{ sec}^{-1}$ ) collisions of polarized protons ( $P=0.7$  in each beam) at collider energies (50 GeV  $\leq \sqrt{s} \leq 500$  GeV) at the Relativistic Heavy Ion Collider (RHIC) at Brookhaven [5]. At the same time, there has also been renewed interest in the subject of the spin content of the proton, motivated by various theoretical analyses [6] of the European Muon Collaboration (EMC) data [7] on the scattering of polarized leptons on polarized nucleons. Some interpretations suggest that a large fraction of the proton spin is carried, not by valence quarks, but by gluons or sea quarks. Such a result has possibly important ramifications for the relevance of a polarization option at future supercolliders where many processes are dominated by sea-quark- or gluon-induced production mechanisms. In any case, the issue of how to measure the longitudinal spin-dependent parton distributions of the proton has received renewed attention in recent studies of various proposed processes, many of which would be accessible at a high luminosity polarized proton-proton collider.

The simplest process which probes the spin-dependent sea-quark distribution is polarized Drell-Yan production and this has been discussed by several groups [8,9]. (The usefulness of Drell-Yan production for probing the *transverse* quark and antiquark distributions of the nucleon, which was first discussed long ago [10], has also recently been “rediscovered” [11] and elaborated upon.) Jet production, both single jet inclusive and dijet events, has been extensively investigated [12–14] and its sensitivity to the polarized gluon distribution discussed using many model parametrizations of the as yet completely unknown  $\Delta G(x, Q^2)$ . [Here  $\Delta G(x, Q^2) = G_+(x, Q^2) - G_-(x, Q^2)$  where  $G_{\pm}(x, Q^2)$  denotes the longitudinal spin-dependent gluon distribution.] Another well-understood collider energy process which is known to depend sensitively on the gluon content of the proton is direct photon production and it has also been intensively

studied [12,15,16] as a probe of  $\Delta G$ . Various proposed RHIC detectors (perhaps with some upgrades) may well be able to detect direct photons with sufficient resolution to make such measurements quite valuable [17].

If some of these processes are used to determine the spin-dependent sea-quark and gluon distributions, it will then be valuable to have additional types of events which can then be used as a further consistency check. In addition, a complete program of spin physics at a polarized collider would also include tests of the spin dependence of the fundamental QCD interactions (once the polarized distributions are measured); this argues for the investigation of the spin dependence of as many additional standard collider processes as possible. The production of three-jet events, for example, has recently been discussed [18], both as an additional testing ground for  $\Delta G$  and for the spin structure of the QCD hard scatterings as well. Two-jet plus photon experiments have been suggested as a further check of the underlying event structure in multi-jet production [19] at unpolarized colliders and the spin dependence of these reactions has also been examined [18]. One final obvious generalization of single direct photon production is double isolated photon production and we will discuss the spin dependence of that process in this article.

This process was first suggested long ago [20] as a probe of quark charges because of contributions from  $q\bar{q} \rightarrow \gamma\gamma$  diagrams [Fig. 1(a)]. It is also known to receive larger contributions [21–23] from the higher-order box diagram [Fig. 1(b)]  $gg \rightarrow \gamma\gamma$ . It has also been discussed by several groups who have examined the possible role of bremsstrahlung diagrams [24–26] and higher-order corrections [27]. In addition, it has been observed experimentally in  $pp$  [28–30] and  $\pi p$  collisions [29,31] and most recently by the Collider Detector at Fermilab (CDF) Collaboration [32] in  $p\bar{p}$  collisions at the Tevatron. So, depending on the kinematic regions probed and applied cuts, this process can probe both the spin-dependent sea-quark and gluon distributions. Another interesting aspect of this process is that it receives an often dominant

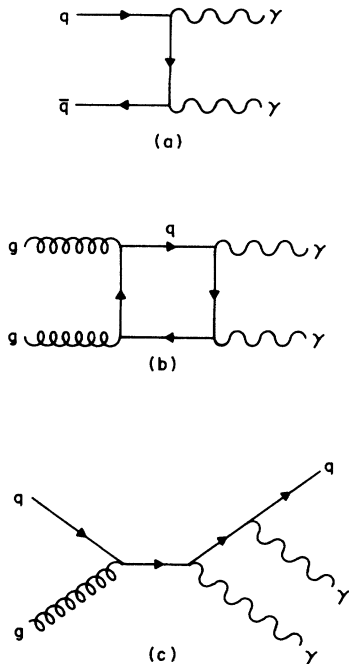


FIG. 1. Typical Feynman diagrams contributing to double photon production, namely (a)  $q\bar{q} \rightarrow \gamma\gamma$ , (b) the box diagram  $gg \rightarrow \gamma\gamma$ , and (c) the single bremsstrahlung diagram  $gg \rightarrow q\gamma\gamma$ .

contribution from a higher-order process (the box diagram  $gg \rightarrow \gamma\gamma$ ) so that it is the first case where one might be directly probing the spin dependence of QCD matrix elements at nonleading order.

Finally, such standard model processes can constitute a background for new processes for which the additional information present in polarized collisions might be used to further enhance the desired signal. For example, two-photon decays of the standard model Higgs boson constitute an important signal for an intermediate mass Higgs scalar and the standard model backgrounds to this process coming from the processes above have been extensively studied [33,34]. Two-photon signals from heavy quarkonium [35] and squarkonium production [36] have also been considered. Motivated by this connection, we also present in Appendix A expressions for the partonic level spin-spin asymmetries for standard model Higgs-boson production via  $gg \rightarrow H^0$  (for low  $p_T$ ) and  $gg \rightarrow gH^0$ ,  $qg \rightarrow qH^0$ , and  $q\bar{q} \rightarrow gH^0$  (high  $p_T$ ).

We begin by considering the various contributions to the unpolarized cross section for isolated double photon production. The two-body subprocesses  $q\bar{q} \rightarrow \gamma\gamma$  and  $gg \rightarrow \gamma\gamma$  automatically yield isolated double photon events. The partonic level cross section for  $q\bar{q} \rightarrow \gamma\gamma$  is given by

$$\frac{d\hat{\sigma}}{d\hat{t}} = \frac{2\pi\alpha^2 e_q^4}{3\hat{s}^2} \left[ \frac{\hat{u}}{\hat{t}} + \frac{\hat{t}}{\hat{u}} \right], \quad (1)$$

where  $e_q$  is the quark charge in units of  $e$ . The one-loop cross section derived from the box diagram for  $gg \rightarrow \gamma\gamma$  is given by (see, e.g., [24] and references therein)

$$\begin{aligned} \frac{d\hat{\sigma}}{d\hat{t}} = & \left[ \sum_q e_q^2 \right]^2 \frac{\alpha^2 \alpha_s^2}{64\pi\hat{s}^2} [5|\mathcal{M}_2|^2 + |\mathcal{M}_1(\hat{s}, \hat{t}, \hat{u})|^2 \\ & + |\mathcal{M}_1(\hat{u}, \hat{t}, \hat{s})|^2 \\ & + |\mathcal{M}_1(\hat{t}, \hat{s}, \hat{u})|^2], \end{aligned} \quad (2)$$

where

$$|\mathcal{M}_2|^2 = 4, \quad (3)$$

$$\begin{aligned} |\mathcal{M}_1(\hat{s}, \hat{t}, \hat{u})|^2 = & \left\{ 2 + 2 \frac{\hat{t} - \hat{u}}{\hat{s}} \ln \left[ \frac{\hat{t}}{\hat{u}} \right] \right. \\ & \left. + \frac{\hat{t}^2 + \hat{u}^2}{\hat{s}^2} \left[ \ln^2 \left[ \frac{\hat{t}}{\hat{u}} \right] + \pi^2 \right] \right\}^2 \end{aligned} \quad (4)$$

and the necessary analytic continuation of  $|\mathcal{M}_1|^2$  gives

$$\begin{aligned} |\mathcal{M}_1(\hat{u}, \hat{t}, \hat{s})|^2 = & \left\{ 2 + 2 \frac{\hat{s} - \hat{t}}{\hat{u}} \ln \left[ \frac{-\hat{s}}{\hat{t}} \right] \right. \\ & \left. + \frac{\hat{t}^2 + \hat{s}^2}{\hat{u}^2} \ln^2 \left[ \frac{-\hat{s}}{\hat{t}} \right] \right\}^2 \\ & + 4\pi^2 \left[ \frac{\hat{s} - \hat{t}}{\hat{u}} + \frac{\hat{t}^2 + \hat{s}^2}{\hat{u}^2} \ln \left[ \frac{-\hat{s}}{\hat{t}} \right] \right]^2. \end{aligned} \quad (5)$$

This expression is derived from earlier calculations of the box diagram for light-by-light scattering [38] and is valid when  $\hat{s}, |\hat{t}|, |\hat{u}| \gg m$  where  $m$  is a constituent quark mass considered in the loop. [We take four effective flavors in our calculations below so that  $(\sum_q e_q^2)^2 = \frac{100}{81}$ .]

It is known that there can be substantial (even dominant) contributions from bremsstrahlung diagrams [24–26,37]. Their effects are largest, however, when one of the radiated photons is collinear with one of the quarks. These contributions can then be highly suppressed by suitable isolation cuts on the photons (i.e., by requiring no hadronic activity near one of the hard  $\gamma$ 's). In addition, the contributions of  $qg \rightarrow q\gamma\gamma$  (and similar double bremsstrahlung contributions) add little new to our knowledge of the polarized parton distributions as they probe almost the identical combination of initial partons as the dominant *single* direct photon subprocess, namely  $qg \rightarrow q\gamma$ . Moreover, the partonic level spin-spin asymmetry for the  $qg \rightarrow q\gamma\gamma$  subprocess, in the limit when one of the photons is collinear with the final state quark, is identical to the asymmetry for the corresponding  $2 \rightarrow 2$  process. [We reproduce the matrix-element and partonic level asymmetry ( $\hat{a}_{LL}$ ) in Appendix B for completeness. Similar limiting cases for other  $2 \rightarrow 3$  cases are illustrated in Ref. [18].] For these reasons, we will assume that it will be possible to apply suitable isolation cuts to effectively eliminate the contributions from bremsstrahlung contributions and we will henceforth consider only the lowest-order  $2 \rightarrow 2$  subprocesses  $q\bar{q} \rightarrow \gamma\gamma$  and  $gg \rightarrow \gamma\gamma$ . This approximation will have to be carefully tested in a full simulation of any proposed RHIC detector which proposes to measure even single direct photon production. (We also leave aside the important question of  $\pi^0/\gamma$  resolution as that will also de-

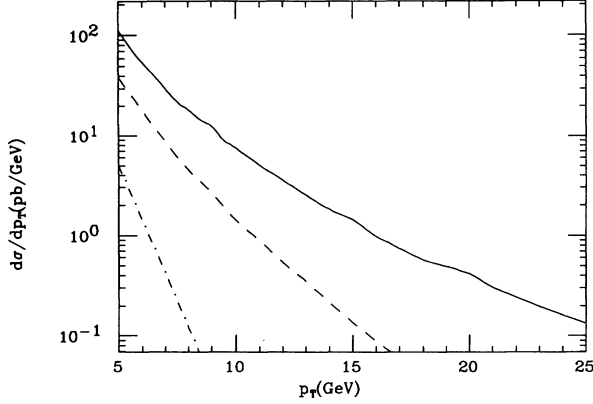


FIG. 2. Differential cross section,  $d\sigma/dp_T$  (pb/GeV) vs  $p_T$  (GeV) for isolated  $\gamma\gamma$  production in  $pp$  collisions based on the  $q\bar{q} \rightarrow \gamma\gamma$  and  $gg \rightarrow \gamma\gamma$  subprocesses. Several possible RHIC center-of-mass energies are shown,  $\sqrt{s} = 500, 150, 50$  GeV (solid, dash, dot-dash).

pend on the detailed experimental situation.)

That this is perhaps not an unreasonable assumption is also suggested by a preliminary analysis of the Tevatron data [32] which impose strong isolation cuts on the photons and then compares the resulting differential cross sections ( $d\sigma/dp_T$  vs  $p_T$ ) versus a PYTHIA Monte Carlo simulation, which includes only the Born and box diagrams, and finds reasonable agreement. We have performed a similar parton level comparison to their data also using only the  $2 \rightarrow 2$  diagrams,  $Q^2 = p_T^2$  as the momentum scale, updated Duke-Owens set I distributions [39], and their stated cuts, and find good agreement (to within 15%) with their PYTHIA Monte Carlo simulation [i.e., Fig. 2(b) of Ref. [32]].

So, using the same set of assumptions, we can estimate the isolated double photon yield in  $pp$  collisions at several RHIC energies and we illustrate the results in Fig. 2. (More specifically we define the variables

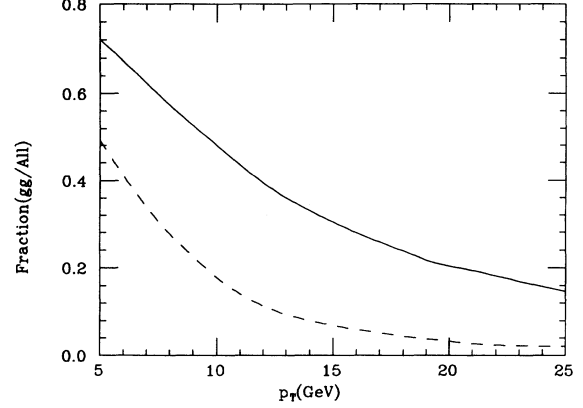


FIG. 3. Fraction of the differential cross section ( $d\sigma/dp_T$ ) arising from gluon fusion (box diagram) contributions vs  $p_T$  for  $\sqrt{s} = 50$  (150) GeV, solid (dash).

$\eta^* = (\eta_1 - \eta_2)/2 = \ln[\cot(\theta^*)]$  and  $\eta_{\text{boost}} = (\eta_1 + \eta_2)/2 = \ln(x_1/x_2)$  where  $\eta_{1,2}$  are the laboratory frame rapidities of the two photons,  $\theta^*$  is the center-of-mass scattering angle of the  $2 \rightarrow 2$  process, and  $x_{1,2}$  are the momentum fractions of the two initial partons. We then insist that  $|\eta^*|, |n_{\text{boost}}| \leq 1.0$  which simulates the CDF cuts [32].) We also plot, in Fig. 3, the fraction of events coming from the box diagram, for two values of  $\sqrt{s}$ , vs  $p_T$ . We see that a substantial part of the total isolated double photon cross section at low transverse momentum arises from purely gluon-induced processes.

To understand the spin dependence of isolated  $\gamma\gamma$  production we require the partonic level longitudinal spin-spin asymmetries:

$$\hat{a}_{LL} = \frac{d\hat{\sigma}(++) - d\hat{\sigma}(+-)}{d\hat{\sigma}(++) + d\hat{\sigma}(+-)}. \quad (6)$$

The observable spin-spin asymmetries  $A_{LL}$  are then given by (e.g., Ref. [40])

$$A_{LL} d\sigma = \sum_{ij} \frac{1}{1 + \delta_{ij}} \int dx_a dx_b [\Delta f_i^{(a)}(x_a, Q^2) \Delta f_j^{(b)}(x_b, Q^2)] \hat{a}_{LL}^{ij} d\hat{\sigma}_{ij}, \quad (7)$$

where  $\hat{a}_{LL}$  denotes the relevant subprocess double helicity asymmetry. The information on the spin-dependent parton distributions is contained in the  $\Delta f(x, Q^2)$  which are defined via

$$\Delta f(x, Q^2) = f_+(x, Q^2) - f_-(x, Q^2) \quad (8)$$

where  $f_+$  ( $f_-$ ) denotes the parton distributions in a polarized nucleon with helicity parallel (antiparallel) to the parent nucleon helicity as mentioned above.

The partonic level asymmetry for the  $q\bar{q} \rightarrow \gamma\gamma$  subprocess is easily seen to be  $\hat{a}_{LL} = -1$  as it is for any purely annihilation process. The  $\hat{a}_{LL}$  for the box diagram process  $gg \rightarrow \gamma\gamma$  can be obtained from a knowledge of the appropriate helicity amplitudes which have been obtained previously [21,22,41]. If we level the parton helicities via  $g(\lambda_1) + g(\lambda_2) \rightarrow \gamma(\lambda_3) + \gamma(\lambda_4)$  we find that the

square matrix elements are proportional to

$$\begin{aligned} (++;++) &= |\mathcal{M}_1(\hat{s}, \hat{t}, \hat{u})|^2, \\ (++;+-) &= |\mathcal{M}_2|^2, \\ (++;-+) &= |\mathcal{M}_2|^2, \\ (++;--) &= |\mathcal{M}_2|^2, \\ (+-;++) &= |\mathcal{M}_2|^2, \\ (+-;+-) &= |\mathcal{M}_1(\hat{u}, \hat{t}, \hat{s})|^2, \\ (+-;-+) &= |\mathcal{M}_1(\hat{t}, \hat{s}, \hat{u})|^2, \\ (+-;--) &= |\mathcal{M}_2|^2, \end{aligned} \quad (9)$$

for the helicity combination labeled  $(\lambda_1, \lambda_2; \lambda_3, \lambda_4)$  plus eight others related by parity. The partonic level asymmetry can then be written as

$$\hat{a}_{LL} = \frac{|\mathcal{M}_2|^2 + |\mathcal{M}_1(\hat{s}, \hat{t}, \hat{u})|^2 - |\mathcal{M}_1(\hat{u}, \hat{t}, \hat{s})|^2 - |\mathcal{M}_1(\hat{t}, \hat{s}, \hat{u})|^2}{5|\mathcal{M}_2|^2 + |\mathcal{M}_1(\hat{s}, \hat{t}, \hat{u})|^2 + |\mathcal{M}_1(\hat{u}, \hat{t}, \hat{s})|^2 + |\mathcal{M}_1(\hat{t}, \hat{s}, \hat{u})|^2}. \quad (10)$$

We plot this asymmetry versus the center-of-mass angle in Fig. 4 and note that it is similar in structure to many of the other  $2 \rightarrow 2$  tree level QCD partonic level spin-spin asymmetries in jet production and single direct photon production. (See Ref. [40] for many examples.)

Given any assumed set of polarized parton distributions we can now predict the observable asymmetry  $A_{LL}$  in a relevant quantity such as  $d\sigma/dp_T$ . We illustrate in Fig. 5 the results for several different parametrizations of the spin-dependent parton distributions which roughly correspond to three extreme cases. The solid curve corresponds to the (pre-EMC) parametrization of Ref. [40] which have a relatively small amount of the proton spin carried by both gluons and sea quarks. In this case, both  $\Delta G$  and  $\Delta s$  are positive so that the very small values of  $A_{LL}$  in this case are also partially due to a cancellation between the negative (positive) contributions from  $q\bar{q}$  ( $gg$ ) initial states. The dash and dot-dash curves correspond to two EMC-motivated sets of distributions used by Cheng and Lai [9,13] which assume a much larger fraction of the proton spin is carried by the gluons and/or sea. The dash (dot-dash) case corresponds to their set  $a$  ( $c$ ) consisting of a large (small)  $\Delta G$  and small (large)  $\Delta s$ . In one case (dash), only the gluon spin contributes ( $\Delta s$  assumed to vanish) and the asymmetry decreases with increasing  $p_T$  due to the diminishing fraction of events induced by gluon fusion. In the dot-dash case, a large (and negative)  $\Delta s$  yields a reasonably large and increasing asymmetry due to the increasing importance of  $q\bar{q}$  initial states and increasing valence quark polarization. The observable asymmetries are not very large except in the case where the sea-quark spin-dependent parton contribution dominates and can suffer from cancellations that may wash out the reasonably large partonic level asymmetries.

We can obtain some rough estimates of the number of

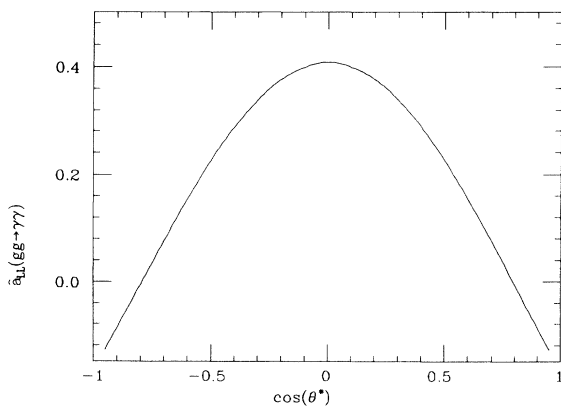


FIG. 4. The partonic level longitudinal spin-spin asymmetry  $\hat{a}_{LL}$  vs  $\cos(\theta^*)$  (where  $\theta^*$  is the center-of-mass scattering angle) for the one-loop process  $gg \rightarrow \gamma\gamma$ . The region of validity of the plot is determined by the conditions  $\hat{s}, |\hat{t}|, |\hat{u}| \gg m$  where  $m$  is a constituent quark mass.

events and the corresponding precision in any asymmetry measurements by assuming two months running time per year (say  $\frac{1}{6} \times 10^7$  sec) with the luminosity mentioned above to obtain  $\approx 330 \text{ pb}^{-1}$  of data which would correspond to  $5.7 \times 10^4$ ,  $6.6 \times 10^3$ ,  $1.6 \times 10^3$  events per year with  $p_T > 5, 10, 15$  GeV, respectively, for  $\sqrt{s} = 500$  GeV. (All this is, of course, before any efficiency, acceptance, or background cuts.) With these event rates the  $1\sigma$  statistical uncertainty in asymmetry measurement will be approximately 1%, 2%, 5% at  $p_T = 5, 10, 15$  GeV making a  $1-2\sigma$  differentiation between the most extreme cases possible, while binning all the data in  $p_T$  would further increase the discrimination power. Clearly, as with all the spin asymmetry measurements foreseen at RHIC, a much more thorough analysis must be made in the context of a realistic RHIC detector. Once again, the desirability of high luminosity for the measurement of (possibly small) asymmetries is evident.

In conclusion, we have discussed the production mechanisms for double isolated photon production at collider energies, concentrating on the two-body subprocesses  $q\bar{q}, gg \rightarrow \gamma\gamma$  as they offer the most *new* information about the spin-dependent parton distributions and QCD matrix elements. We have derived the partonic level asymmetries and illustrated some expectations for observable double longitudinal asymmetries using sample spin-dependent sea-quark and gluon parton distributions.

Many of the processes discussed so far for study at a polarized collider have only been considered at leading order (as we have done above and in the Appendixes) and, ultimately, full next-to-leading-order calculations will be required for the systematic extraction of spin-dependent parton distributions and the precise testing of

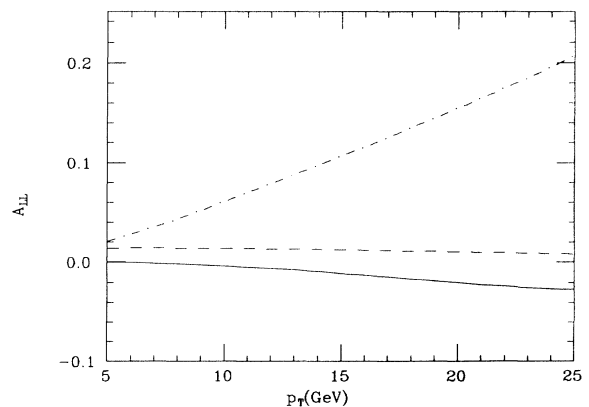


FIG. 5. Longitudinal spin-spin asymmetry  $A_{LL}$  in the quantity  $d\sigma/dp_T$  vs  $p_T$  (GeV) for various assumed spin-dependent sea-quark and gluon parton distributions. The plot is for  $pp$  collisions at  $\sqrt{s} = 500$  GeV. The solid curve corresponds to the small  $\Delta s$  and  $\Delta G$  of Ref. [40]. The dashed (dot-dashed) curves correspond to the large (small)  $\Delta G$  and small (large)  $\Delta s$ , set  $a$  ( $c$ ) of Refs. [9,13].

the spin structure of the basic QCD interactions. A few examples of calculations of radiative corrections for the relevant spin-dependent processes exist in the literature, namely for Drell-Yan [42] and (single) direct photon production [43], and methods now exist which may greatly facilitate the calculations for more complex processes [44]. Clearly, more work will be needed (and performed) once the prospect of sufficient data exists to warrant the effort.

One of us (R.R.) thanks the Phenomenology Institute of the University of Wisconsin and Argonne National Laboratory, where part of this work was carried out, for their hospitality. This work was supported in part by the National Science Foundation under Grant No. PHY-9001744 (R.R.), by the Texas National Research Laboratory Commission (R.R.), by the University of Wisconsin Alumni Research Foundation (M.D.), by the U.S. Department of Energy under Contract No. DE-AC02-76ER00881 (M.D.), and by the Texas National Research Laboratory Commission under Grant No. RGFY9173 (M.D.).

#### APPENDIX A

Thus far, we have concentrated on the derivation of the spin dependence of the standard model QCD matrix elements which produce isolated  $\gamma\gamma$  pairs. It was pointed out above that this final state is also important as a possible signature of an intermediate mass Higgs boson. Therefore, it may be of some relevance to collect the appropriate cross sections and partonic level spin-spin asymmetries for both low and high transverse momentum Higgs-boson production here as well. Higgs-boson production in these two kinematic regions has been extensively discussed (see, e.g., [45,46]) and we will make extensive use of existing results. (The QCD corrections to the most important of these Higgs production processes have very recently been calculated [47] but the spin dependence has not been investigated as yet.)

The  $2 \rightarrow 1$  process,  $gg \rightarrow H^0$ , proceeding via a triangle diagram, gives rise to low transverse momentum Higgs-boson production. Ellis *et al.* [45] give the invariant amplitude for  $gg \leftrightarrow H^0$  from which one can easily derive the partonic level asymmetry, namely

$$\hat{a}_{LL}(gg \rightarrow H^0) = +1, \quad (\text{A1})$$

$$\frac{d\hat{\sigma}}{d\hat{t}}(gg \rightarrow g^1 S_0) = \frac{\pi\alpha_s^3 R_0^2}{2M\hat{s}^2} \frac{(\hat{s}^4 + \hat{t}^4 + \hat{u}^4 + M^8)(\hat{s}\hat{t} + \hat{t}\hat{u} + \hat{u}\hat{s})^2}{(\hat{s}\hat{t}\hat{u})[(\hat{s}-M^2)(\hat{t}-M^2)(\hat{u}-M^2)]^2}, \quad (\text{A5})$$

$$\frac{d\hat{\sigma}}{d\hat{t}}(qg \rightarrow q^1 S_0) = -\frac{2\pi\alpha_s^3 R_0^2}{9M\hat{s}^2} \frac{\hat{u}^2 + \hat{s}^2}{\hat{t}(\hat{t}-M^2)^2}, \quad (\text{A6})$$

$$\frac{d\hat{\sigma}}{d\hat{t}}(q\bar{q} \rightarrow g^1 S_0) = \frac{16\pi\alpha_s^3 R_0^2}{27M\hat{s}^2} \frac{\hat{t}^2 + \hat{u}^2}{\hat{s}(\hat{s}-M^2)^2}, \quad (\text{A7})$$

where  $R_0$  is the quarkonium radial wave function evaluated at the origin. Much of this similarity is dictated by the common helicity structure of the two classes of processes, with the complication of the bound state nature of

which has been previously derived by Bourrely *et al.* [40]. The effective two-gluon coupling of the Higgs boson, generated by the effective Lagrangian

$$\mathcal{L}_{\text{eff}} \sim G^{\mu\nu\alpha} G_{\mu\nu\alpha} H,$$

is of exactly the same form as that for the two gluon coupling of a  $^1S_0 Q\bar{Q}$  bound state and yields the same helicity structure as that for  $gg \leftrightarrow ^1S_0$ , which can be derived using the helicity amplitudes in the collection of Gastmans and Wu [48]. [The partonic level asymmetries for  $gg \rightarrow ^3P_0, ^3P_2$  quarkonium production are similarly large [48,49] as  $\hat{a}_{LL}(gg \rightarrow ^3P_0/^3P_2) = +1/-1$  and this is easily understood by simple conservation law arguments.]

Thus, the  $gg \rightarrow H^0$  partonic level asymmetry is maximal and one can imagine looking for structure in the spin-spin asymmetry of the two-photon invariant mass distribution as an additional tool for an intermediate mass Higgs-boson search, or, perhaps, for a heavy  $\eta(Q\bar{Q})$  quarkonium or squarkonium state. This is akin to the use of single spin asymmetries in the search for standard or new  $W$  or  $Z$  bosons via their two-jet decays [12,14]. The usefulness of this technique, of course, depends critically on the size of the, as yet unmeasured, spin-dependent gluon distribution,  $\Delta G(x, Q^2)$ .

The matrix elements for the leading order  $O(\alpha_s^3)$   $2 \rightarrow 2$  processes,  $gg \rightarrow gH^0$ ,  $qg \rightarrow qH^0$ , and  $q\bar{q} \rightarrow gH^0$  are quite complicated functions of  $M_H$ ,  $M_{\text{top}}$ , and the kinematic variables  $\hat{s}$ ,  $\hat{t}$ , and  $\hat{u}$  [45,46] but do take on a simple form in the limit that the top-quark mass is large compared to all other mass scales, i.e., when  $M_{\text{top}}^2 \gg \hat{s}, \hat{t}, \hat{u}, M_H^2$ . In that case one finds that the invariant matrix elements

$$\sum |\mathcal{M}(gg \rightarrow gH^0)|^2 = \frac{32\alpha_s^3 \alpha_W}{3} \frac{(\hat{s}^4 + \hat{t}^4 + \hat{u}^4 + M_H^8)}{\hat{s}\hat{t}\hat{u}M_W^2}, \quad (\text{A2})$$

$$\sum |\mathcal{M}(qg \rightarrow qH^0)|^2 = -\frac{16\alpha_s^3 \alpha_W}{9} \frac{\hat{u}^2 + \hat{s}^2}{\hat{t}M_W^2}, \quad (\text{A3})$$

$$\sum |\mathcal{M}(q\bar{q} \rightarrow gH^0)|^2 = \frac{16\alpha_s^3 \alpha_W}{9} \frac{\hat{t}^2 + \hat{u}^2}{\hat{s}M_W^2}. \quad (\text{A4})$$

In this limit, the similarity to  $^1S_0$  production at large  $p_T$  is again apparent as evidenced by the corresponding cross sections for quarkonium production [48,50], i.e.,

the quarkonium state responsible for the additional complexity. One can make use of the expansion of the amplitudes of Ellis *et al.* [45] in terms of invariant functions or the explicit helicity amplitudes of Baur and Glover [46]

in this limit to calculate the spin-spin asymmetries and we find that

$$\hat{a}_{LL}(gg \rightarrow gH^0) = \frac{M^8 + \hat{s}^4 - \hat{t}^4 - \hat{u}^4}{M^8 + \hat{s}^4 + \hat{t}^4 + \hat{u}^4}, \quad (\text{A8})$$

$$\hat{a}_{LL}(qg \rightarrow qH^0) = \frac{\hat{s}^2 - \hat{u}^2}{\hat{s}^2 + \hat{u}^2}, \quad (\text{A9})$$

$$\hat{a}_{LL}(q\bar{q} \rightarrow gH^0) = -1. \quad (\text{A10})$$

As expected from the similar helicity structure, the spin-spin asymmetries for the corresponding  $^1S_0$  high  $p_T$  production processes are identical [48,51]. We plot in Fig. 6 examples of the asymmetries in (A8) and (A9) versus the center-of-mass angle for two values of  $\sqrt{\hat{s}}/M_H$  for illustration.

For high  $p_T$  Higgs boson plus jet production, followed by the  $H^0 \rightarrow \gamma\gamma$  decay, the backgrounds would arise from  $q\bar{q} \rightarrow g\gamma\gamma$  and  $qg \rightarrow q\gamma\gamma$  final states plus, of course, three-jet events with two jets misidentified as photons.

## APPENDIX B

In this appendix, we list, for completeness, the squared matrix element for the single bremsstrahlung process  $qg \rightarrow q\gamma\gamma$  and the corresponding partonic level longitudinal spin-spin asymmetry. Using the results of Ref. 48 we find that the matrix element, squared, and summed (averaged) over initial (final) spins and colors is given by

$$|\overline{\mathcal{M}}|^2 = \frac{8}{3} q^2 e_q^4 (p \cdot p') \times \frac{\sum_{i=1}^3 (p \cdot k_i)(p' \cdot k_i)[(p \cdot k_i)^2 + (p' \cdot k_i)^2]}{\prod_{i=1}^3 (p \cdot k_i)(p' \cdot k_i)}, \quad (\text{B1})$$

where the process is labeled by

$$q(p) + g(k_1) \rightarrow q(p') + \gamma(k_2) + \gamma(k_3).$$

The partonic level asymmetry can then be derived using the explicit helicity amplitudes of Ref. [48] and we find

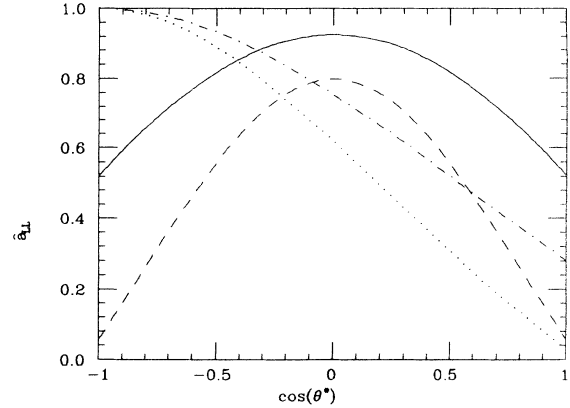


FIG. 6. Partonic level asymmetries  $\hat{a}_{LL}$  vs  $\cos(\theta^*)$  for  $gg \rightarrow gH^0$  for  $\sqrt{\hat{s}} = 2(6)M_H$ , solid (dash) and for  $qg \rightarrow qH^0$  for  $\sqrt{\hat{s}} = 2(6)M_H$ , dot-dash (dot).

$$\hat{a}_{LL} = \frac{H_{++} - H_{+-}}{H_{++} + H_{+-}}, \quad (\text{B2})$$

where

$$H_{++} = (p \cdot k_3)(p' \cdot k_3)^3 + (p \cdot k_2)(p' \cdot k_2)^3 + (p' \cdot k_1)(p \cdot k_1)^3, \quad (\text{B3})$$

$$H_{+-} = (p \cdot k_3)^3(p' \cdot k_x) + (p \cdot k_2)^3(p' \cdot k_2) + (p' \cdot k_1)^3(p \cdot k_1). \quad (\text{B4})$$

One can then see that in the limit where one of the final state photons is collinear with the quark this asymmetry reduces to the corresponding expression for the  $2 \rightarrow 2$  process,  $qg \rightarrow q\gamma$ , namely (cf. Ref. [40]),

$$\hat{a}_{LL} = \frac{\hat{s}^2 - \hat{u}^2}{\hat{s}^2 + \hat{u}^2}. \quad (\text{B5})$$

Thus, the bremsstrahlung contributions offer little new information on the spin dependence of the basic QCD interactions that is not contained in the single direct photon production.

- [1] See, e.g., S. Y. Lee and E. D. Courant, Phys. Rev. D **41**, 292 (1990), and references therein; Brookhaven Report No. AD/RHIC-63 (unpublished).
- [2] *Polarized Collider Workshop*, Proceedings, University Park, Pennsylvania, 1990, edited by J. Collins, S. Heppelmann, and R. W. Robinett, AIP Conf. Proc. No. 223 (AIP, New York, 1991).
- [3] S. Y. Lee, in *Polarized Collider Workshop* [2], p. 30.
- [4] See A. D. Krisch *et al.*, Phys. Rev. Lett. **63**, 1137 (1989), for the first experimental tests of the Siberian snake concept. See also A. D. Krisch, in *Polarized Collider Workshop* [2], p. 13.
- [5] For a review of the prospects for a program of polarized  $pp$  collisions at RHIC, see D. Underwood, A. Yokosawa, G. Bunce, Y. Makdisi, M. Tannenbaum, S. Y. Lee, R. L. Jaffe, J. Collins, S. Heppelmann, and R. W. Robinett, Par-

ticle World (to be published).

- [6] See, e.g., R. L. Jaffe and A. Manohar, Nucl. Phys. **B337**, 509 (1990); A. Manohar, in Ref. [2], p. 90; A. Efremov, in *Polarized Collider Workshop* [2], p. 80.
- [7] EMC Collaboration, J. Ashman *et al.*, Phys. Lett. B **206**, 364 (1988); Nucl. Phys. **B328**, 1 (1989).
- [8] J. C. Collins, in *Proceedings of the Workshop on Hadron Structure Functions and Parton Distributions*, edited by D. Geesaman, J. Morfin, C. Sazama, and W.-K. Tung (World Scientific, Singapore, 1990), p. 378.
- [9] H.-Y. Cheng and S.-N. Lai, Phys. Rev. D **41**, 91 (1990).
- [10] J. Ralston and D. Soper, Nucl. Phys. **B152**, 109 (1979).
- [11] R. L. Jaffe and X. Ji, Phys. Rev. Lett. **67**, 552 (1991).
- [12] C. Bourrely, J. Ph. Guillet, and J. Soffer, Nucl. Phys. **B361**, 72 (1991).
- [13] H.-Y. Cheng, S.-R. Hwang, and S.-N. Lai, Phys. Rev. D

- 42, 2243 (1990).
- [14] J. Ph. Guillet, in *Polarized Collider Workshop* [2], p. 155; G. Nardulli, *ibid.* p. 196.
- [15] E. L. Berger and J. Qiu, *Phys. Rev. D* **40**, 778 (1989); J. Qiu, in *Polarized Collider Workshop* [2], p. 162; see also Cheng and Lai [9].
- [16] S. Gupta, D. Indumathi, and M. V. N. Murthy, *Z. Phys. C* **42**, 493 (1989); E. Richter-Was, *Acta Phys. Pol.* **B15**, 75 (1984).
- [17] A. Yokosawa, D. Underwood, and K. Enyo (private communications).
- [18] M. A. Doncheski, R. W. Robinett, and L. Weinkauff, *Phys. Rev. D* **44**, 2717 (1991).
- [19] V. Barger, T. Han, J. Ohnemus, and D. Zeppenfeld, *Phys. Lett. B* **232**, 371 (1989). See also S. Keller and J. F. Owens, *ibid.* **266**, 126 (1991).
- [20] S. M. Berman, J. D. Bjorken, and J. B. Kogut, *Phys. Rev. D* **4**, 3388 (1971); K. Soh, P. Y. Pac, H. W. Lee, and J. B. Choi, *ibid.* **18**, 751 (1978); M. Krawegky and W. Ochs, *Phys. Lett.* **79B**, 119 (1978).
- [21] B. L. Combridge, *Nucl. Phys.* **B174**, 243 (1980).
- [22] A. Carimalo, M. Crozon, P. Kessler, and J. Parisi, *Phys. Lett.* **98B**, 105 (1981).
- [23] Ll. Ametller, E. Gava, N. Paver, and D. Treleani, *Phys. Rev. D* **32**, 1699 (1985).
- [24] E. L. Berger, E. Braaten, and R. D. Field, *Nucl. Phys.* **B239**, 52 (1984).
- [25] A. P. Contogouris, L. Marleau, and B. Pire, *Phys. Rev. D* **25**, 2459 (1982).
- [26] A. P. Contogouris, N. Mebarki, and H. Tanaka, *Phys. Rev. D* **35**, 1590 (1987).
- [27] P. Aurenche, A. Douiri, R. Baier, M. Fontannaz, and D. Schiff, *Z. Phys. C* **29**, 459 (1985).
- [28] AABC Collaboration, C. Kourkoumelis *et al.*, *Z. Phys. C* **16**, 101 (1982).
- [29] NA3 Collaboration, J. Badier *et al.*, *Phys. Lett.* **164B**, 184 (1985).
- [30] AFS Collaboration, T. Åkesson *et al.*, *Z. Phys. C* **32**, 491 (1986).
- [31] WA70 Collaboration, E. Bonvin *et al.*, *Phys. Lett. B* **236**, 523 (1990); *Z. Phys. C* **41**, 591 (1989).
- [32] CDF Collaboration, R. Harris, in *The Vancouver Meeting—Particles and Fields '91*, Proceedings of the Joint Meeting of the Division of Particles and Fields of the American Physical Society and the Particle Physics Division of the Canadian Association of Physicists, Vancouver, 1991, edited by D. Axen, D. Bryman, and M. Comyn (World Scientific, Singapore, 1992), p. 719.
- [33] H. Baer and J. F. Owens, *Phys. Lett. B* **205**, 377 (1988).
- [34] D. A. Dicus and S. D. Willenbrock, *Phys. Rev. D* **37**, 1801 (1988); J. F. Gunion, G. L. Kane, and J. Wudka, *Nucl. Phys.* **B299**, 231 (1988).
- [35] V. Barger, E. W. N. Glover, K. Hikasa, W.-Y. Keung, M. G. Olsson, C. J. Suchyta III, and X. Tata, *Phys. Rev. D* **35**, 3366 (1987); **38**, 1632(E) (1988).
- [36] P. Moxhay and R. W. Robinett, *Phys. Rev. D* **32**, 300 (1985); M. J. Herraro, *Phys. Lett. B* **200**, 205 (1986).
- [37] R. Ghandi, F. Halzen, and F. Herzog, *Phys. Lett.* **152B**, 261 (1985).
- [38] B. DeTollis, *Nuovo Cimento* **32**, 753 (1964); **35**, 1182 (1965).
- [39] J. F. Owens, *Phys. Lett. B* **266**, 126 (1991); D. W. Duke and J. F. Owens, *Phys. Rev. D* **30**, 49 (1984).
- [40] C. Bourrely, J. Soffer, F. M. Renard, and P. Taxil, *Phys. Rep.* **177**, 319 (1989).
- [41] K. Kajantie and R. Raitio, *Phys. Lett.* **87B**, 133 (1979); see also R. N. Cahn and J. F. Gunion, *Phys. Rev. D* **20**, 2224 (1979).
- [42] P. Ratcliffe, *Nucl. Phys.* **B223**, 45 (1983).
- [43] S. Papadopoulos, A. Contogouris, and F. V. Tkachov, in *The Vancouver Meeting—Particles and Fields '91* [32], p. 621.
- [44] Z. Bern and D. A. Kosower, *Phys. Rev. Lett.* **66**, 1669 (1991); see also Z. Bern and D. A. Kosower, in *Polarized Collider Workshop* [2], p. 358, for a calculation of the one-loop corrections to the  $gg \rightarrow gg$  helicity-dependent cross sections; D. Kosower, *Phys. Lett. B* **254**, 434 (1991).
- [45] R. K. Ellis, I. Hinchliffe, M. Soldate, and J. J. Van Der Bij, *Nucl. Phys.* **B297**, 221 (1988).
- [46] U. Baur and E. W. N. Glover, *Nucl. Phys.* **B339**, 38 (1990).
- [47] A. Djouadi, M. Spira, and P. M. Zerwas, *Phys. Lett. B* **264**, 440 (1991).
- [48] R. Gastmans and T. T. Wu, *The Ubiquitous Photon* (Oxford University Press, Oxford, England, 1990).
- [49] M. A. Doncheski and R. W. Robinett, *Phys. Lett. B* **248**, 188 (1990).
- [50] R. Baier and R. Rückl, *Z. Phys. C* **19**, 251 (1983).
- [51] R. W. Robinett, *Phys. Rev. D* **43**, 113 (1991).